Running head: AUDITORY ROTATING ELLIPSE SHAPE PERCEPTION

Squeaky Wheels: Auditory Perception of Rotating Ellipse Shape from Friction-generated Sound

Patrick A. Cabe

University of North Carolina at Pembroke

Katharina S. Bochtler and John G. Neuhoff

The College of Wooster

AUTHOR SUBMITTED COPY

Author Note

Patrick A. Cabe, Department of Psychology, University of North Carolina at Pembroke; Katharina S. Bochtler, Department of Psychology, The College of Wooster; John G. Neuhoff, The College of Wooster.

We gratefully acknowledge the financial support of The College of Wooster.

Correspondence concerning this article should be directed to Patrick A. Cabe, 924 Fearrington Post, Pittsboro, NC 27312. E-mail: patrick.cabe@uncp.edu

Abstract

Acoustical analysis indicates that sounds generated as the rims of ellipses rotate against a fixed contactor specify ellipse shapes (minor-to-major axis length ratios), potentially supporting human ability to perceive the shapes. In 4 experiments, we documented human ability to differentiate and scale ellipse shape from friction-generated sound. All four experiments yielded clear evidence of ability to differentiate and scale ellipse shape. Experiment 1 demonstrated reliable and ordinally correct shape judgments. Experiment 2 showed equivalent judgments over rotation speeds (10, 15, 20 rpm), suggesting reliance on relational information in the acoustic signal. Experiment 3 (scalar judgments) and Experiment 4 (multiple-choice judgments) tested perceptual learning effects. Some improvement occurred in both experiments, with a moderate advantage for multiple-choice judgments. Individual variability was notable across all experiments: Individual correlations (actual vs. judged shape) ranged from .00 to > .9. Past research revealed perception of shape from impact noise; the current experiments are the first apparent demonstrations of human ability to perceive planar object shape from friction-generated sound. Results are interpreted as consistent with Gibson's theory of information-based perception.

Key words: shape perception; auditory perception; shape from motion

Public Significance Statement: From squeaky wheels to squeaky hinges to squeaky shoes, friction-generated sounds are facts of everyday life. While impact sounds are known to support perception of object properties – particularly object shape – no parallel ability to use friction-generated sound to perceive object shape has apparently ever been discovered. We report that human listeners can reliably discriminate and scale ellipse shapes, based on the frictional sounds made as ellipse rims rotated against a contactor. Sensitivity to friction-generated sound may be useful for interpreting mechanical events, but, more generally, our results indicate another dimension of the richness of the human acoustic environment.

Squeaky Wheels: Auditory Perception of Rotating Ellipse Shape from Friction-generated Sound

Humans routinely perceive object shapes via vision and touch, but the possibility that acoustic information might support auditory object shape perception remains arguable. Research on shape from sound began with work on echolocation in bats (Griffin, 2001), which showed that bats locate and identify varying shapes using self-emitted reflected ultrasonic clicks. Rosenblum and Robart (2007) presented evidence that human observers can use ambient acoustic information to perceive shapes of sound-obstructing objects in expansive environments. Additionally, broad environmental shapes are of interest with respect to wayfinding by vision-impaired individuals. Neuhoff (2001) provided a review of the literature relevant to both auditory wayfinding and impending listener-object interactions.

However, some authors have been pessimistic about the possibility of auditory perception of discrete object shapes. In a widely cited perspective on auditory information for shape, Kac (1966) asked: “Can one hear the shape of a drum?” Kac concluded that the resonant properties of a tapped drum head would not, in fact, support discrimination of drum head shapes, even given perfect acoustic transmission and a perfect ear. Nevertheless, special cases exist in which Kac’s conjecture is true (e.g., triangles, Grieser & Maronna, 2013; trapezoids, Hezari, Lu, & Rowlett, 2016).

Kac’s (1966) work and subsequent analyses focused on impact sound (e.g., discrete taps). In studies of shape perception from sound, perceptual researchers typically have also studied responses to acoustic signals generated by impacts on objects. Comprehensive reviews of the relevant literature (Gaver, 1988, 1993a, b; Giordano, 2005; Kirkwood, 2007) summarize the

studies on auditory shape perception, particularly from impacts, as well as perceptual consequences associated with other environmental sound sources. Briefly, from those reviews, some studies show clear evidence for shape discriminations and identifications, while others are less compelling.

Comparatively few empirical perceptual studies have directly examined shape from sound, and as far as we have been able to find, tests of perception of shape from sound have almost exclusively employed impact sound. Lakatos, McAdams, and Caussé (1997) discovered that participants reliably discriminated relative heights and widths of equal-length wooden or metal blocks using the acoustic signal produced by tapping the blocks with a mallet. Houix, McAdams, and Caussé (1999) examined variations in the position at which the mallet struck metal bars differing in geometry. Houix et al. found that participants appeared predominantly to match pitch, regardless of the object's shape.

Kunkler-Peck and Turvey (2000) pursued Kac's (1966) question more directly, proposing that acoustic properties of a vibrating object depend on its geometry and material. They, therefore, restated Kac's query in terms of the height and width of a thin vibrating plate. Analysis of the plates' vibratory modes following discrete impacts implied the existence of information about plate geometry. Results of four experiments clearly revealed that participants discriminated height and width of rectangular plates, base length versus altitude of triangular plates, and diameters of circular plates. Participants also correctly reported the plate material (wood, steel, or acrylic).

Sounds emerge from a wide variety of environmental events, including striking (as in studies cited above), rolling (Houben, Kohlrausch, & Hermes, 2004), splashing (cf., Cabe & Pittenger, 2000), crumpling (Bresin, Delle Monache, Fontana, Papetti, Polotti, & Visell, 2008),

and others (cf., Gaver, 1993a, b). As a loose generalization, environmental sounds commonly originate from only limited event categories: (a) impacts, as in hammering; (b) vibrating objects, such as a tuning fork; (c) perturbations in a stream of flowing air, as in whistling; and (d) friction, as in a door squeaking. Quite widely, in everyday experience, we associate sounds with frictional events (Akay, 2002). The immediate focus of our research was on friction-generated noise from objects, within a defined shape class (ellipses), rubbing against another object.

A notable insight in previous research on shape from sound is that stimuli were generally constrained to families of shapes. We elected to study only ellipse shapes, for several reasons. First, ellipse shapes are readily defined by a single shape parameter. We operationalized shape as the relationship of the minor axis length to the major axis length, expressed as a percentage. Second, the mathematics of ellipses is well known and accessible, allowing the derivations shown in the Appendix. Third, the shape parameter range, conveniently, is constrained to values between zero and 1.00. Fourth, ellipses are completely convex, with no concavities in their perimeters. Thus, as a practical benefit, the perimeter of the ellipse could slide continuously and smoothly past the contactor we used to generate frictional sound. By contrast, polygons have discontinuities where their sides intersect, so it is difficult to maintain constant mechanical contact between ellipse perimeters and contactor.

Apparently, little perceptual work has been done with friction-generated sounds. The only examples we have found are recent studies by Thoret and colleagues (Thoret, Aramaki, Kronland-Martinet, Velay, & Ystad, 2014; Thoret, Aramaki, Bringoux, Ystad, & Kronland-Martinet, 2016). Pointing out that (visual) shape is not usually associated with sounds, Thoret et al. (2014) had participants match four shapes (line patterns) displayed on a computer screen with auditory patterns based on recordings either of pen friction across a tablet or of similar

synthesized sounds, made as if a pen traced the shapes. Two of the patterns were an ellipse and a circle (i.e., an ellipse with equal major and minor axis lengths). While Thoret et al. (2014) do not give the actual sizes of the visual patterns, measurements of the figure in the paper suggest the ellipse had a minor-to-major axis length ratio of approximately 0.3 – 0.4, and the circle's diameter was approximately equal to the ellipse major axis length. Confusion matrices showed clear evidence of differentiation of the patterns. In particular, with respect to the work reported here, participants differentiated the circle and the ellipse.

In a second series of experiments, Thoret et al. (2016) asked participants to draw a circle or ellipse, while listening to either congruent (circle-circle, ellipse-ellipse) or incongruent (circle-ellipse) audio recordings of synthesized sounds approximating friction-generated acoustic patterns from the trajectory of a pen moving over a tablet. A primary finding was that the incongruent sound patterns biased the drawings in the direction of the auditory pattern, suggesting sensitivity to the auditory shape. Interestingly, the shapes participants drew, even in the congruent circle-circle condition, were all somewhat biased toward an elliptical shape.

While clearly relevant to the experiments reported here, Thoret et al. (2014, 2016) employed quite a narrow range of stimulus patterns. Specifically, in a forced choice task, they presented four visual patterns, including only one circle and only one ellipse, with the ellipse having a particular minor-to-major axis ratio. Consequently, the degree to which perceivers might use acoustic information to differentiate and to scale ellipse shapes remains unknown. Further Thoret et al. (2014, 2016) reported only group data. Thus, individual differences cannot be discerned from their data.

Theoretical context

Kac's (1966) mathematical approach is reminiscent of J. Gibson's (1966, 1979) theory of ecological perception, which posits that all perception depends on the structure of stimulus arrays. Several authors (Sedgwick (1973; see also Turvey, Solomon, & Burton, 1989; Cabe, 2011; Cabe & Hofman, 2012) have described basic principles of the ecological perception research program: (a) Discover potentially informative structure in stimulus arrays; (b) test organismic sensitivity to the array information; and (c) where perceptual performance is relatively inaccurate or unreliable, apply perceptual learning manipulations to test for improvement in such performance. That is the pattern we followed in the present set of experiments.

It is useful to be explicit about what constitutes stimulus array information. Assume some environmental property is to be perceived, a property that is not itself immediately represented in the stimulus array. If physical properties of the array are causally contingent (via the laws of physics) on that environmental property, then stimulus array information for that property exists. Often, both the environmental property and the properties of the stimulus array can be described in physical-mathematical terms. If those physical-mathematical descriptions can be connected (e.g., by an equation), that relationship defines the stimulus array description as information for the environmental property. Alternatively, if physical-mathematical descriptions of a changing environmental property vary in some regular fashion, and the physical-mathematical descriptions of the stimulus array vary in parallel with those of the environmental property, we can claim that information exists for the set of changes in the environmental property in the set of varying stimulus array changes (as exemplified in the Appendix). To support perception, stimulus array properties must be available to a perceiver's perceptual systems. Relevant stimulus array properties become available to the perceiver via transformations of stimulus array properties

emerging from the perceiver's exploration or via events involving the environmental property. Such changes may be described using derivatives of stimulus array variables. A critical assumption is that perceivers are sensitive to such progressive changes.

J. Gibson (1966; see also Michaels & Carello, 1981) asserted that perception is direct, requiring no cognitive amendments (e.g., memory, inference). Cabe (2010, 2011, 2013; Cabe & Hofman, 2012) has argued that the use of novel tasks is important for tests of the Gibsonian position. As Aurell (1984) pointed out, tasks that are closely related to everyday activities, and are therefore highly practiced, may depend on memory, rather than (or in addition to) more immediate stimulus array information, and therefore may be indistinguishable from direct perception.

In passing, we suggest the possibility that participants in the experiments of Thoret et al. (2014, 2016), all of whom may reasonably be assumed to be experienced users of writing instruments, may have come to tacitly associate certain sound patterns with particular drawing movements and thus may have been able to apply such incidental learning to the experimental tasks required. By contrast, the experimental stimulus materials and the tasks reported here were quite unfamiliar, likely completely outside participants' experience. Consequently, learned associations between the friction-generated sound patterns we presented and object shape are highly improbable as an explanation of shape differentiation and scaling. Because the task was novel, the positive shape from sound results we report here support Gibson's direct perception theory and the ecological research program.

Relation to visual shape from motion

The visual perception literature documents that the motions of objects, particularly rotations, reveal their shapes (see, e.g., reviews in Lappin, 1995; Todd, 1995). In particular, deforming boundaries or contours available as an object rotates allow reliable percepts of the three-dimensional shape of objects. Norman, et al. (2016) and Wong (2001) provide useful historical perspectives.

Although some theoretical analyses exist to show how deforming boundary contours (silhouettes) of objects might yield perception of three-dimensional shape (e.g., Wong, 2001), the issue remains something of an open question (see Norman et al., 2016). One approach to modeling three-dimensional shape in terms of two-dimensional boundary deformations is to consider the 3-D shape as a series of thin stacked plates (e.g., Bocheva, 2009; Egan, Todd, & Phillips, 2011; McCrae, 2014). Then any given point on the deforming contour can be described in terms of that point's changing distance from the 3-D object's axis of rotation.

Applying that conception to acoustic events, we considered the fact that, for a planar object rotating at a fixed speed, the pattern of friction-generated sound varied with the distance between the center of rotation and the contact point on the perimeter of the planar shape. With a constant rotation speed, changes in the friction-generated sound are causally related to the distance of the contact point from the shape's center of rotation, so changes in friction-generated sound patterns as the object rotates are information for the shape of the planar object. The analysis in the Appendix makes this point quite clear. What is missing is the demonstration that human listeners can actually use such information to perceive shape.

Scope of the research

We report here four experiments. In all of them, we asked participants to judge ellipse shape based on recordings of friction-generated sounds made as the rotating ellipses rubbed against a contactor. We varied ellipse shape by fixing the major axis length and adjusting minor axis lengths to specified proportions of the major axis length. The minor axis length as a percentage of the major axis length, then, is a convenient shape parameter. In Experiment 1, with a single rotation speed, we demonstrated that humans can perceive ellipse shape from such friction-generated sound. In Experiment 2, we varied rotation speed, to replicate and extend the first experiment. In Experiment 3, we gave participants feedback on judgment accuracy and looked for improvements in performance. Experiment 4 repeated the perceptual learning manipulation, but with a different response mode (multiple-choice among several alternatives vs. scalar estimation). In both Experiments 3 and 4, we also tested transfer to novel rotation speeds. Surprisingly, across all four experiments, participants reliably differentiated ellipse shapes and scaled the ellipses appropriately on a group basis. In addition, a majority of participants showed significant correlations between actual and estimated ellipse shapes.

General Methods

Participants

We recruited participants via the Amazon Mechanical Turk (AMT) network for each of the experiments reported here. Previous work demonstrates that AMT samples have reliability that is as good as, or better than, that obtained from traditional undergraduate samples (Buhrmester, Kwang, & Gosling, 2011; Holden, Dennie, & Hicks, 2013; Paolacci, Chandler, & Ipeirotis, 2010). Moreover, traditional attention and psychophysical tasks have been well replicated with AMT participants. Those experiments include the Stroop effect, flanker task, Simon effect, attentional blink, task switching, inhibition of return, masked priming, change

deafness, and auditory motion perception (Crump, McDonnell, & Gureckis, 2013; Neuhoff, 2016; Neuhoff, Schott, Kropf, & Neuhoff, 2014).

None of our participants reported hearing difficulties. All were naïve with respect to the purposes of the experiment. Participants received $0.30 (US) for their participation through the AMT system. All procedures were approved by The College of Wooster's Human Subjects Research Committee. We affirm that participants were tested in accord with standard ethical guidelines.

Sample Size

We conducted an *a priori* power analysis using G*Power 3.1 (Faul, Erdfelder, Buchner, & Lang, 2009) and subsequently set sample sizes for Experiments 2-4 at $N = 126$ (42 participants per group x 3 groups). This yielded a power of .82 to detect a moderate effect size ($f = .2$) at an alpha level of .05 for the between-groups measure of a mixed design ANOVA with three between-groups and seven repeated measures. We used $N = 42$ in Experiment 1 (which had no between-groups manipulation) to allow appropriate comparisons with subsequent experiments. Power for all within-groups and interaction effects exceeded that of the between-groups portion of the ANOVA.

Apparatus and materials

Ellipses. We tested seven ellipses with minor axis lengths of 30, 40, 50, 60, 70, 80, and 90 percent of a fixed major axis length (8 in.; 20.3 cm). Ellipses were 10-gauge (0.104-in. thick) sheet steel. A hole at the geometric center of each ellipse allowed a 1 1/2 in. x 5/16 in. bolt to be inserted and secured with a lock washer and nut. We deburred sharp edges of the ellipses using a hand file.

Rotation apparatus. We mounted a variable-speed electric motor on the back of a vertical 3/4 in.-thick plywood panel, with the motor shaft protruding through the panel. The panel was screwed to a base made of 2 x 10 lumber, and to triangular braces between the base and the panel. We clamped the panel assembly firmly to a heavy workbench.

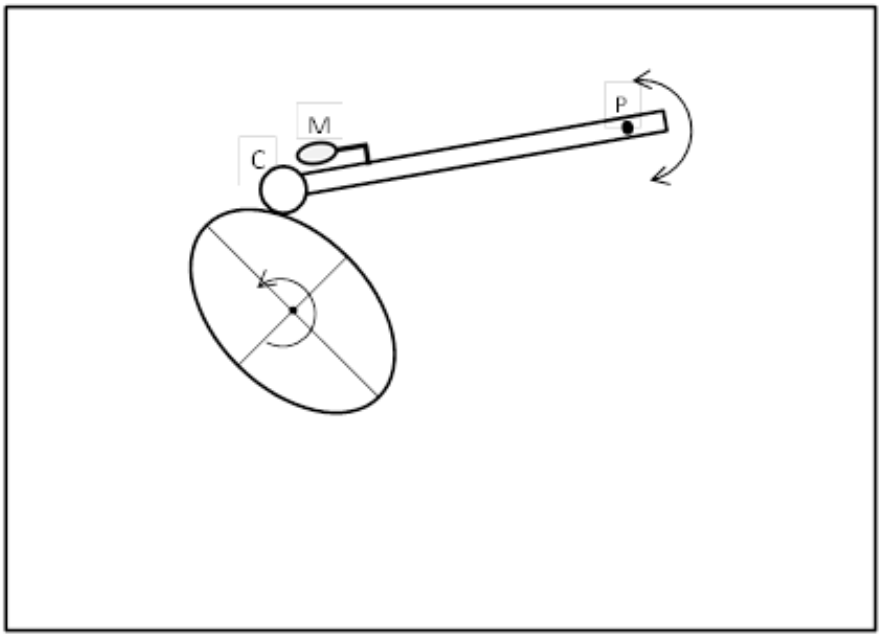

Figure 1. Schematic diagram of the recording apparatus. An ellipse attached to the shaft of a motor rotated against a contactor (C), attached to an arm, which pivoted via a ball bearing connection (P), with the contactor in constant contact with the rotating ellipse. A microphone (M), attached to the pivoting arm, picked up the sound made as the ellipse rubbed against the contactor.

The bolt through the center of each ellipse threaded into collar attached to the motor shaft. Power to the motor ran through an on-off switch, then through the speed controller. Thus, once the speed was set, the switch controlled the operation of the motor. Prior to making recordings, we set the motor's rotation speed by attaching a circular disk to the motor shaft, starting the motor, counting rotations for 30 sec, and then calculating rotation speed. We used rotation speeds of 10, 15, and 20 rpm.

Figure 1 depicts the general layout of the recording setup. A pivoting wooden arm (33 cm long x 3 cm wide x 0.8 cm thick) was attached to the panel supporting the motor. The pivot was located 22 cm to the right of, and 17 cm above, the motor shaft. The pivot was a 4 1/2 in. x 1/4 in. diameter bolt firmly attached to the plywood panel. The bolt went through two small ball bearings fixed to the pivoting arm, resulting in a freely moving, quiet, and relatively rigid attachment of the arm to the panel.

Screwed to the end of the arm was a contactor, made of a 5 cm length of 1 1/2-in. (3.8 cm) diameter wooden dowel. Two cylindrical neodymium magnets (1/2 in. diameter x 1/2 in. length) inserted into a hole drilled into the end of the contactor provided some mass and a small magnetic attraction, both of which helped maintain the contactor's contact with the rotating ellipses.

When the apparatus operated, the rotating ellipse rubbed on a strip of 220 grit sandpaper wrapped around the contactor. The contactor and ellipse were osculating figures, with only one point of contact at their common tangent point.

The weight of the pivot arm and contactor against the ellipse was approximately constant at about 80 g, measured with the arm at approximately the level of the minimum arm declination (i.e., when the major axis of the ellipse would be horizontal). The ellipses rotating against the sandpaper-covered contactor produced a sound center, modulated as a function of the distance of the contact point from the axis of rotation, against a raspy background. To the experimenter's ear, different ellipses produced sounds that differed.

Recording devices. A small microphone (removed from a discarded computer voice-recognition system; model and characteristics unknown) was attached to the pivoting arm. The microphone head was approximately 5 cm from the contact point between the contactor and the

ellipse. The microphone was connected to a small digital recorder (Olympus VN-722PC; Olympus America, Inc., Center Valley, PA).

Recording procedure

Recording took place in a quiet space. To avoid possible discriminative cues from adventitious extraneous noises on the recordings, we recorded multiple samples at different times for each of the ellipses. For each recording, an ellipse was threaded onto the motor shaft, and the recorder started. The experimenter orally indicated the ellipse number, speed, sample designation), waited for a few seconds and then paused the recorder. The contactor at the end of the pivoting arm was then placed against the rim of the ellipse and the motor started, and the recorder was restarted; recording continued for approximately 1 min. Recordings were digitized at a sampling rate of 44.1 kHz, and saved as 320 kbps mp3 files (as required by the AMT on-line presentation system). Files were then organized into the sequences used in participant testing.

Figure 2 shows example waveforms and spectrograms for 30%, 60%, and 90% ellipses. Those were respectively the smallest, middle, and largest ellipse shape values we tested. Although the sound stimuli are generally noisy, distinct frequency and amplitude modulation becomes more apparent as the ellipses become narrower. Spectral peaks coincide with the rotation of the ellipse and are more distinct with narrower ellipses.

Figure 2. Waveform of the 40% minor-to-major axis length ellipse rotating against a fixed contactor at 20 rpm. The horizontal axis is time in seconds; the vertical axis is relative sound intensity.

Stimulus presentations

Because rotation speeds differed in Experiments 2, 3, and 4, how to manage trial length was an important consideration. If trial length was defined as a particular time interval, then the number of rotations participants heard would differ for different rotation speeds. With trial length limited to a fixed number of rotations, the time per trial would differ for different rotation speeds. Seeing no clear way to avoid the issue, we elected the latter procedure, restricting each trial to three complete rotations of the ellipse. We acknowledge the potential confound and address it in the General Discussion.

Experiment 1: Ellipse differentiation and scaling

Friction-generated sound is a function of the contact force between two surfaces, the contact area, the surface properties of the apposed surfaces, and the relative velocities of the surfaces against each other (see Appendix). We arranged for ellipses, rotating about their centers, to rub against a non-rotating contactor covered with sandpaper. Thus, contact area, contact forces, and surface roughness were essentially constant. Hence, the major source of variation in the frequency and intensity of the friction-generated noise was the tangential velocity of the ellipse at the point of contact with the contactor. For a constant angular velocity (rotation speed), tangential velocity was a function of the distance of the contact point from the center of the ellipse. That distance varied regularly with ellipse dimensions, greatest at the ends of the major axis and least at the ends of the minor axis. That is, tangential velocity varied with the ratio of minor axis length to major axis length, a convenient index of ellipse shape (see Figure A1).

The analysis in the Appendix, supported by visual examination of waveforms and spectrograms from the recordings used (e.g., see Figure 2), indicated that sound patterns vary

regularly with ellipse shape. The first approximation analysis in the Appendix suggests that sound frequency and intensity change from relative maxima (as the ends of the ellipse major axes pass the contactor) to relative minima (as the ends of ellipse minor axes pass the contactor). When ellipses rotate at a constant speed, rates of change between frequency-intensity maxima and minima also vary as a function of ellipse shape.

Figure A1, which assumes equal angular velocities, makes this clear. Because all the ellipses exemplified in Figure A1 have the same length major axes, absolute maximum tangential velocities are equal. But tangential velocity minima differ markedly as a function of ellipse shape, with those minima *directly* proportional to their minor-to-major axis length ratios. The rates of change of tangential velocities are *inversely* proportional to the minor-to-major axis length ratios (see Figure A2). Because friction-generated sound is a function of tangential velocity against the contactor, information exists in those rates of change for differing ellipse shape.

In Experiment 1, rotation speed during recording was constant at 20 rpm. Participants listened to the recorded friction-generated sounds from ellipses differing in shape and made shape judgments using a slider on a visual analog scale. We predicted that (a) participants would differentiate the ellipses reliably and (b) participants' shape judgments would reliably track actual ellipse shapes.

Method

Participants

Participants came from the AMT service (N = 42, ages 21 – 62 years, median, 30; 22 female).

Apparatus and Materials

Participants listened to stimulus recordings prepared as described above, using their own personal devices. Participants heard two sound samples for each of the seven ellipses (minor axis lengths 30, 40, 50, 60, 70, 80, and 90% of major axis length), for a total of 14 trials. Visual displays were also via participants' own devices. Participants responded by adjusting the position of a slider horizontally along an on-screen visual analog scale that was marked with nine ellipses with minor axis lengths ranging from 20 to 100% of the major axis length (see Figure 3). Recordings did not include the 20% and 100% alternatives; those were presented to reduce central tendency biases.

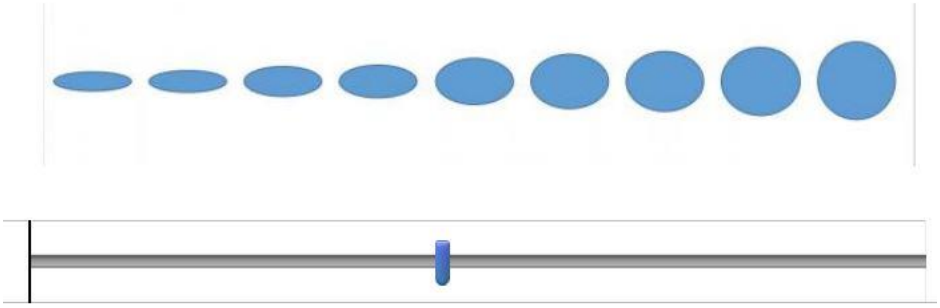

Figure 3. Sliding response mechanism and visual analog scale used in Experiment 1. Pictured ellipses have minor axis lengths that range from 20% (far left ellipse) to 100% (far right ellipse) of the (constant) major axis. Participants adjusted the position of the slider to indicate the perceived shape of the ellipse making the sound that they heard.

Procedure

After providing informed consent, participants heard oral instructions to adjust their listening device to a comfortable level. To verify that they could actually hear the sound, they typed a spoken code word into a text box on the screen. They were then instructed that they

would hear a series of sounds made by the edge of a rotating disk rubbing against a contactor. Participants saw a silent video clip of the apparatus used to produce the sound. Participants were then instructed to adjust the slider to indicate their estimate of the ellipse shape.

Results and Discussion

The slider scale displayed ellipses with minor-to-major axis lengths ranging from 20 to 100%, and the software recorded values corresponding to the proportional distance along the slider scale (0 – 100% of the distance between 20 and 100%). Consequently, we rescaled actual slider settings to the 20 to 100% range for analysis.

We analyzed rescaled judgments, averaged over the two samples for each ellipse, in a one-way repeated measures ANOVA. The Ellipse effect was significant, $F(6, 246) = 10.00$, $p < .001$, $\eta_{part}^2 = .20$. The linear trend was also significant, $F(1, 41) = 17.72$, $p < .001$, $\eta_{part}^2 = .30$.

Pairwise comparisons among the seven ellipses showed that 16 of 21 mean differences were significant (uncorrected for multiple comparisons), $t(41) = 2.22$ to 5.03, $p = .034$ to $< .001$, Cohen's $d = 0.34$ to 0.78. Not surprisingly, significant differences occurred primarily with the greatest shape differences. Figure 4 shows the group average curve for Experiment 1.

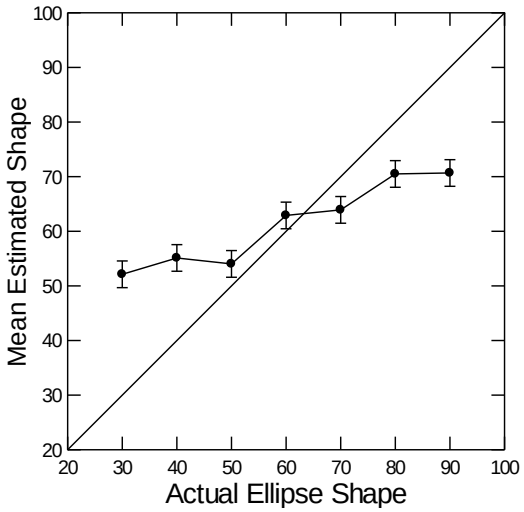

Figure 4. Mean shape from sound judgments for ellipses in Experiment 1. The diagonal line represents perfect performance. Error bars are ± 1 *SEM*, calculated by the method of Franz and Loftus (2012).

Individual correlation[1] magnitudes between actual and estimated ellipse shape parameters ranged from .005 to .86 (median, .61; n = 14 data points; 2 samples x 7 ellipses per participant). Among those, 25 of 42 (60%) were significant ($p < .05$), with 3 of 25 negative. Similar significant but negative effects have been reported in other studies, particularly with relatively unfamiliar tasks (e.g., Cabe, 2010; Withagen & Caljouw, 2011).

The combination of the significant ANOVA effect for ellipse shape, the significant linear trend, and the set of significant pairwise mean judgment differences converge on the conclusion that human participants reliably differentiated and scaled ellipse shapes using friction-generated acoustic information. Individual differences were evident, however. Most of the participants

[1] The correlation magnitudes reported are somewhat tentative approximations, because they do not take into account repeated measures across ellipses. We acknowledge the violation of the assumption of independence of measures. Although techniques exist for accounting for intra-individual correlations across repeated measures, there were too few measures in the present data set to support such an analysis. We do remark that the lack of independent observations is mitigated to a degree by the fact that presentation of the stimulus recordings was randomized. Thus, while individual sensitivities no doubt varied, it was not possible to predict from one trial to the next what the stimulus ellipse actually was. Further, group correlation magnitudes between judgments for the seven ellipses averaged only r = .29, suggesting that the influence of judgments of one ellipse on judgments of other ellipses was not great.

made shape judgments with reasonable to excellent reliability; others seemed unable to do the task at all. The origins of those individual differences warrant additional research.

Experiment 2: Rotation Speed Comparison

Experiment 1 demonstrated the basic effect that human listeners could use friction-generated sounds to differentiate and scale ellipse shapes, for a single rotation speed. In Experiment 2, we expanded the range of speeds. If the absolute differences between maxima and minima are usable information, shape judgments should be equivalent across speeds, because absolute maxima and minima are constant, and minima differ by ellipse shape, at any rotation speed. Again, we predicted that (a) participants would differentiate the ellipses reliably and (b) participants' shape judgments would reliably track actual ellipse shapes.

Method

Participants

Participants (N = 126; ages 18 to 67 years, median, 29.5; 71 male) came from the AMT system. We assigned individuals randomly in equal numbers (n = 42) to three rotation speed groups: 10 rpm, 15 rpm, or 20 rpm. Subgroups did not differ significantly in age or gender.

Stimulus Materials

We used recordings made as described in the General Methods section. Participants listened to two samples of each of the seven ellipse shape recordings (14 trials total).

Procedure

The procedure used in Experiment 1 was also followed in Experiment 2, with the exception of rotation speed differences.

Results and Discussion

As in Experiment 1, we rescaled shape estimates to values within the range of ellipse shapes displayed on the slider scale (20 – 100% minor-to-major axis lengths), and then averaged judgments over the two samples for each ellipse. We analyzed the averaged rescaled values in a 7 (ellipses) x 3 (rotation speeds: 10, 15, 20 rpm) ANOVA, with Rotation speed as a between-subjects factor. The Ellipse main effect was again significant, $F(6, 738) = 20.13$, $p < .001$, $\eta_{part}^2 = .14$. The Rotation speed main effect, however, was not significant, $F < 1.00$, *ns*, $\eta_{part}^2 = .01$, nor was the interaction, $F < 1.00$, *ns*, $\eta_{part}^2 = .01$.

As in Experiment 1, the linear trend for Ellipse was significant, $F(1, 123) = 48.12$, $p < .001$, $\eta_{part}^2 = .28$. Paired comparisons among ellipses (including all participants, because speeds showed no difference) indicated that mean judgments for 15 of the 21 pairs differed significantly, $t(125) = 2.23$ to 6.70, $p = .028$ to $< .001$, Cohen's $d = 0.20$ to 0.60. Bonferroni-corrected values indicated significant differences for 13 of 21 pairs.

Correlation magnitudes (actual vs. estimated shape) for individuals ($n = 14$ data points; 2 samples x 7 ellipses) ranged from .005 to .94 (median, .49). Of the 126 participants, 60 (48%) showed significant correlations ($p < .05$). Four individuals showed significant, but negative, correlations. Figure 5 shows the group average curves for Experiment 2.

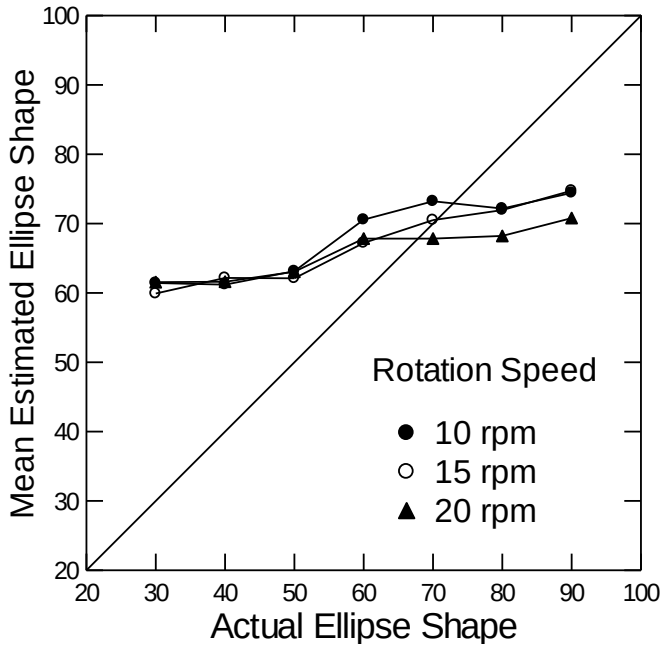

Figure 5. Mean judged ellipse shape (minor axis length as a percentage of major axis length) versus actual shape in Experiment 2. Because judgments did not differ across the three rotation speeds, we averaged judgments across speeds. The diagonal line represents perfect performance. Error bars are omitted for clarity. The three speeds did not differ significantly.

The outcomes of Experiment 2 are quite consistent with those of Experiment 1. Notably, the results for the 20 rpm group specifically replicated the results of Experiment 1. On a group basis, the significant linear trend and the significant pair-wise mean differences further indicated that participants effectively differentiated and scaled ellipse shape. Individual differences, again, were prominent.

Experiment 3: Perceptual Learning with Scalar Judgments

The first two experiments documented human ability to differentiate and scale ellipse shape from friction-generated sound patterns. In both experiments, individual performances ranged from random to highly reliable. Figures 4 and 5 show participants overestimated low shape values and underestimated high shape values, a pattern termed the *regression effect*

Stevens (1975) and *regression bias* by Gescheider (1997). Those outcomes suggest that performances might be improved by perceptual learning, specifically practice with feedback on judgment accuracy.

Following the theoretical perspective of E. Gibson (1969), Cabe and Wagman (2010) proposed that evidence for the effects of perceptual learning on scalar judgments can be seen in changes in regression statistics: Increasing r^2 values indicate greater variance accounted for in perceptual judgments by actual stimulus values, implying improved stimulus differentiation; regression slopes approaching unity and regression intercepts approaching zero both imply improved judgment accuracy relative to actual scalar values.

Cabe and Wagman (2010) developed a Perceptual Calibration Index (PCI) as a measure of the state of perceptual performance. Linear regression for scalar perceptual measurements against physical scalar values yields a correlation (the squared value of which is the variance in the perceptual response accounted for by the stimulus variable), a regression slope, and a regression intercept. Those three values define a point in a three-dimensional state space, with ideal perceptual performance represented by the point at which variance accounted for is 1.00, the slope is 1.00, and the intercept is zero.

In the state space, the geometric distance between the point representing current performance and the point representing ideal performance defines the PCI, calculated using the formula:

$$PCI = \sqrt{(1 - r^2)^2 + (1 - |C_1|)^2 + (\|C_2\|)^2}$$

where r^2 is variance accounted for, $|C_1|$ is the absolute value of the regression slope and $\|C_2\|$ is the regression intercept normalized to the largest value within the set of perceptual judgments over which the regression was calculated. Perfect performance yields a PCI of zero; random

performance yields a PCI of 1.5 (a zero correlation, a zero slope, and an intercept with a normalized value of .5).

Decreasing PCI values across blocks of trials, then, indicate perceptual learning. We applied the PCI technique to the data collected in the present experiment.

Further, E. Gibson (1969) proposed that, if perceptual learning yields enhanced sensitivity to stimulus array invariants, then such learning should transfer to new, untrained stimulus events in which those same invariants occur. In the present work, we surmised that the relevant invariant information is the pattern of change between frequency-intensity peaks at the ends of ellipse major axes (constant for all ellipses, because all had the same major axis length) and the troughs at the ends of ellipse minor axes (varying regularly with ellipse shape). Therefore, experience with one speed of rotation might transfer to other untrained speeds.

Rates of change between maxima and minima also vary across ellipse shapes. Those rates of change are specific to ellipse shape, but only if angular velocities (rotation speeds) are equal. However, tangential velocity, on which friction-generated sound depends, is a function both of angular velocity and distance between the ellipse center and the contact point. Thus, altering rotation speed also alters tangential velocity and the rates of change between maxima and minima, raising the possibility that shape judgments could be affected by rotation speed.

Participants practiced judging ellipse shape from friction-generated sound at one rotation speed, with feedback on accuracy, and then (without feedback) made judgments under either the same or different speeds. If reinforced practice improved participants' sensitivity to the relevant acoustic information for ellipse shape, then they should (a) exhibit improved judgments over trials with feedback on accuracy; (b) show persistent ability to make such judgments under the training rotation speed, in the absence of feedback; and (c) transfer (show equivalent

performance) to new rotation speeds. As in Experiments 1 and 2, we expected that ellipses would be reliably differentiated and scaled.

Method

Participants

Participants were 126 (47 female) volunteers from the AMT network, aged 18 to 66 years (median, 31), randomly assigned in equal numbers (n = 42) to three transfer speed groups: 10 rpm, 15 rpm, and 20 rpm. Transfer speed groups were statistically equivalent in gender distribution and mean age.

Materials

Training phase. During training with feedback, all participants heard recordings made using ellipses rotating at 15 rpm. Ellipses had minor-to-major axis length percentages of 30, 40, 50, 60, 70, 80, and 90 (the same values used in Experiments 1 and 2).

Transfer phase. Participants heard recordings for the same ellipses as in the training phase, made at rotation speeds of 10, 15, or 20 rpm. The 15 rpm recordings were the same as those used during the training phase.

Procedure

Training phase. Participants completed three blocks of training trials. Each block presented recordings of each of the seven ellipses, in random order. As in Experiments 1 and 2, participants adjusted a slider to the point on the scale that best represented the shape of the ellipse they heard (see Figure 3). After each shape judgment, the computer screen showed (a) the participant's judgment and (b) a graphic of the ellipses with a pointer indicating the correct ellipse (see Figure 6).

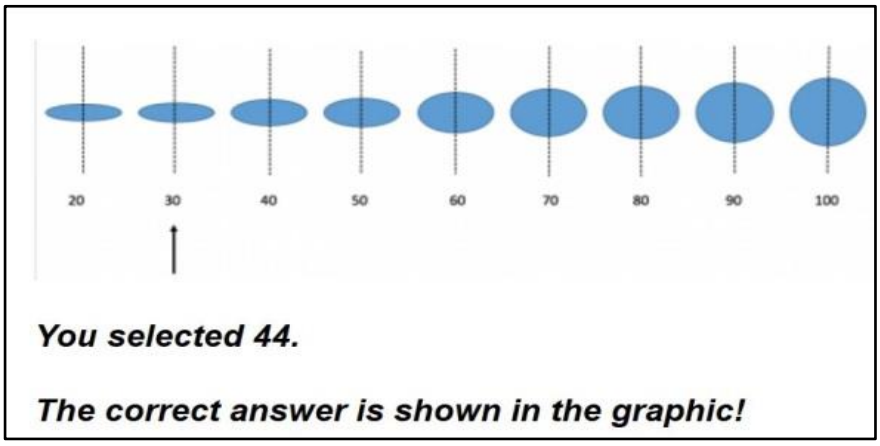

Figure 6. Example of the feedback graphic used in Experiment 3.

Transfer phase. The procedure for the transfer phase was the same as for the training phase, except that participants heard recordings made at either 10, 15, or 20 rpm, with 10 and 20 rpm the novel speeds. Participants received no feedback in the transfer trials.

Results and Discussion

Initial analysis

After rescaling as previously described, we analyzed judgments from the entire experiment in an initial 2 (phase: training, transfer) x 7 (ellipses) x 3 (trial blocks) x 3 (transfer speeds) ANOVA, with repeated measures over Phases, Ellipses, and Blocks. Results showed significant main effects for Phase, $F(1, 123) = 4.85$, $p = .03$, $\eta_{part}^2 = .04$; for Ellipses, $F(6, 738) = 131.53$, $p < .001$, $\eta_{part}^2 = .52$; and for Block, $F(2, 246) = 3.89$, $p = .02$, $\eta_{part}^2 = .03$; but not for Transfer speed, $F < 1.00$, *ns*, $\eta_{part}^2 = .01$. Globally, those outcomes are consistent with our expectations.

Significant interactions occurred for Phase x Ellipse, $F(6, 738) = 3.95$, $p = .001$, $\eta_{part}^2 = .03$, and for Block x Ellipse, $F(12, 1476) = 4.06$, $p < .001$, $\eta_{part}^2 = .03$. The Phase x Ellipse x Block interaction was significant, $F(12, 1476) = 2.71$, $p = .001$, $\eta_{part}^2 = .02$, but none of the other interactions were. Significant interactions appeared to be due to the large degrees of freedom, rather than any useful effect. Figure 7 shows the relationship between actual and estimated shape for the training phase (with feedback on judgment accuracy) and transfer (with no feedback).

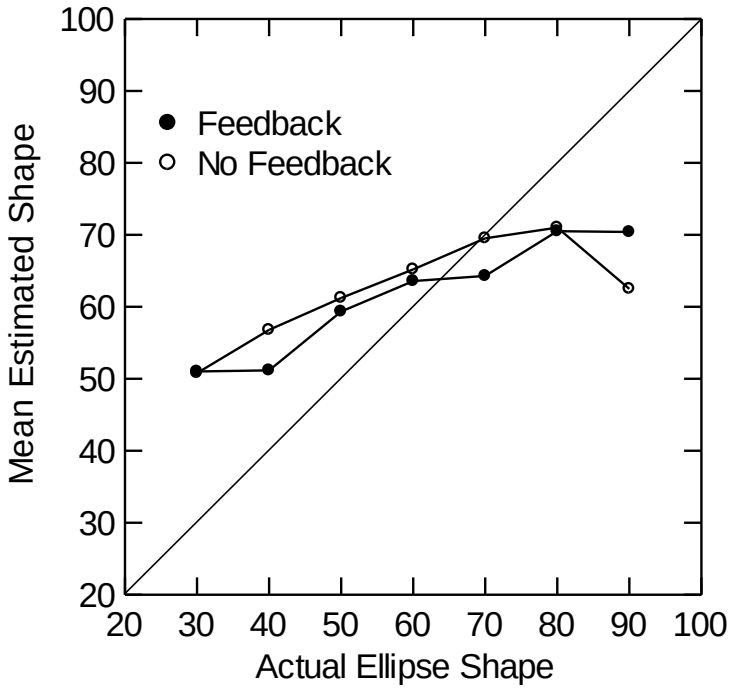

Figure 7. Mean judged ellipse shape versus actual shape in Experiment 3. Data from all speed comparison groups are combined. Error bars are omitted because SEMs calculated using the method of Franz and Loftus (2012) fall within the size of the plotted points. The diagonal line represents perfect performance.

Because phases differed, we analyzed Training and Transfer data separately, in separate 7 (ellipse) x 3 (block) x 3 (transfer speed) ANOVAs. Transfer speed was a between-groups factor.

Training phase

As in Experiments 1 and 2, the only significant main effect was for Ellipse, $F(6, 738) = 89.02$, $p < .001$, $\eta_{part}^2 = .42$. As predicted, Transfer speed groups did not differ, $F < 1.00$, *ns*, $\eta_{part}^2 = .003$. Somewhat surprisingly, there was also no difference across Blocks, $F(2, 246) = 1.89$, $p = .15$, $\eta_{part}^2 = .02$. Only the Ellipse x Block interaction was significant, $F(12, 1476) = 5.38$, $p < .001$, $\eta_{part}^2 = .04$.

As before, there was a strongly significant linear trend for Ellipse, $F(1, 123) = 279.74$, $p < .001$, $\eta_{part}^2 = .84$. Pair-wise comparisons of mean judgments showed 18 of 21 significant, Bonferroni-corrected $t(125) = 3.71$ to 14.80, $p = .007$ to $< .001$, Cohen's $d = 0.33$ to 1.32. These outcomes replicate those from Experiments 1 and 2.

Individual correlation magnitudes ($n = 21$ data points; 7 ellipses x 3 blocks) between actual and judged ellipse shape ranged from .00 to .89 (median, .49); 77 (61%) were significant ($p < .05$). All of the significant correlations were positive.

Transfer phase

The Transfer phase ANOVA again showed a significant main effect for Ellipse, $F(6, 738) = 81.38$, $p < .001$, $\eta_{part}^2 = .40$, but not for Block, $F(2, 246) = 1.74$, $p = .18$, $\eta_{part}^2 = .01$. Importantly, the Transfer speed main effect was not significant, $F(2, 123) = 1.96$, $p = .15$, $\eta_{part}^2 = .03$, nor was any interaction involving Transfer Speed. Both the non-significant Transfer speed main effect and non-significant interactions with Transfer speed support the inference that the experience in the Training phase persisted with new rotation speeds.

The linear trend for the Ellipse factor was strongly significant: $F(1, 123) = 203.25$, $p < .001$, $\eta_{part}^2 = .88$. In pair-wise mean judgment comparisons (including all participants, because transfer speed groups did not differ), 18 of 21 pairs were significant, Bonferroni-corrected $t(125)$

= 3.83 to 13.45, p = .004 to < .001, Cohen's d = 0.34 to 1.20. We conclude that participants, as a group, both reliably differentiated and scaled ellipse shapes.

Individual correlation magnitudes (n = 21) ranged from .01 to .91 (median, .51); 76 (60%) were significant ($p < .05$), with none of the significant correlations negative.

PCI analysis

Using the Cabe and Wagman (2010) method, we calculated PCI values for each participant for each block in the two experimental phases of Experiment 3 and tested those values in a 3 (transfer speeds) x 3 (blocks) ANOVA, with repeated measures over blocks. We analyzed Training and Transfer phases separately.

Training phase. Training phase data yielded a significant main effect only for Block, $F(2, 246) = 19.51$, $p < .001$, $\eta_{part}^2 = .14$. Because participants received feedback on judgment accuracy, we expected blocks to differ, but the pattern of means was less orderly than anticipated: Significant pairwise differences occurred between Training blocks 1 (M = 1.13, SD = 0.36) and 2 (M = 0.86, SD = 0.46), $t(125) = 6.15$, $p < .001$, Cohen's d = 0.55, and between Training blocks 2 and 3 (M = 1.06, SD = 0.42), $t(125) = 4.38$, $p < .001$, Cohen's d = 0.39. However, Training blocks 1 and 3 did not differ, $t(125) = 1.57$, p = .12, Cohen's d = 0.14. That pattern of differences leaves the effects of the feedback unsettled.

Transfer phase. The Transfer phase yielded a small main effect for Transfer speed, $F(2, 123) = 3.28$, p = .04, $\eta_{part}^2 = .05$. PCI values did not differ significantly across Blocks, $F < 1.00$, *ns*, $\eta_{part}^2 = .001$. The interaction was non-significant, $F(4, 246) = 1.32$, p = .26, $\eta_{part}^2 = .02$. Pair-wise comparisons among Tranfer speed mean judgments revealed that values for the 10 rpm group (M = 1.08, SD = 0.36) were significantly higher than those for the 20 rpm group (M = 0.88, SD = 0.38), $t(82) = 2.50$, p = .014, Cohen's d = 0.27. The 10 rpm group did not differ

significantly from the 15 rpm group (M = 0.92, SD = 0.40), $t(82) = 1.91$, $p = .06$, Cohen's d = 0.21, nor did the 15 rpm group differ from the 20 rpm group, $t(82) = 0.51$, $p = .61$ Cohen's d = 0.06. Why the 10 rpm group performed less well than the 20 rpm group is not apparent, although it is possible that the rate of change at that slowest rotation speed may not have supported shape judgments so well as faster speeds, so that feedback was less effective. The issue requires additional study.

To summarize, Experiment 3 again indicated that participants reliably differentiated and scaled ellipse shape from friction-generated sound. There was some indication of change across trial blocks under feedback and some indication that performance persisted with changed rotation speeds. While the perceptual learning results are a bit ambiguous, the results of Experiment 3 reinforced the conclusion that friction-generated sound patterns can inform ellipse shape judgments, replicating Experiments 1 and 2.

Experiment 4: Perceptual Learning with Multiple-choice Judgments

Experiment 3 used scalar judgments of the ellipse shape parameter, and the perceptual learning manipulation yielded only a moderate indication of improvement. Further, individual differences were still notable: About 40% of the participants never showed a significant correlation between actual and judged ellipse shape. Even among those who made reliable judgments, regression slopes remained generally low, with regression intercepts still substantially higher than zero. Evidently, there was yet room for improvement in ellipse shape perceptual performance.

Consequently, we arranged Experiment 4 to be simpler than Experiment 3. The procedure in Experiment 4 paralleled that in Experiment 3, with three important exceptions: First, rather

than a scalar judgment, participants made discrete (multiple choice) judgments by selecting the number of the ellipse that they perceived as having been used to make a given recording, by referring to a graphical display of numbered ellipses. Second, we reduced the ellipse shape choices from nine to seven, all of which actually occurred in the stimulus set (in Experiment 3, the end points, 20 and 100, were not in fact presented). Third, feedback during training was specific and precise, giving the participant the exact number of the correct ellipse shape.

As in Experiment 3, we expected to find that perceptual performance improved over the training trial blocks, that performance would be maintained from training trials to transfer trials, and that transfer would occur to novel transfer test speeds. As in Experiment 3, we tested those hypotheses both on the actual judgments and using the Cabe and Wagman (2010) PCI approach.

Method

Participants

We recruited 126 volunteers from the AMT network; ages ranged from 19 to 68 years (median, 31); 57 were women. As in Experiment 3, participants were assigned to three transfer speed groups (10, 15, and 20 rpm; $n = 42$ each). Transfer speed groups did not differ significantly in gender distribution or mean age.

Materials

We used the same recordings as in Experiment 3. Recordings were for ellipses with minor-to-major axis length percentages of 30, 40, 50, 60, 70, 80, and 90.

Procedure

The training and transfer phases were the same as those used in Experiment 3, except for the participant's response mechanism. Instead of a scalar response, participants selected the ellipse that they thought was used to make the sound by clicking a box directly below one of

seven ellipses (labeled 1-7) displayed on their computer screen. After each judgment, the screen graphic gave participants feedback on the accuracy of that judgment with the same visual display of ellipses and an added verbal message indicating both their choice and the correct choice (see Figure 8).

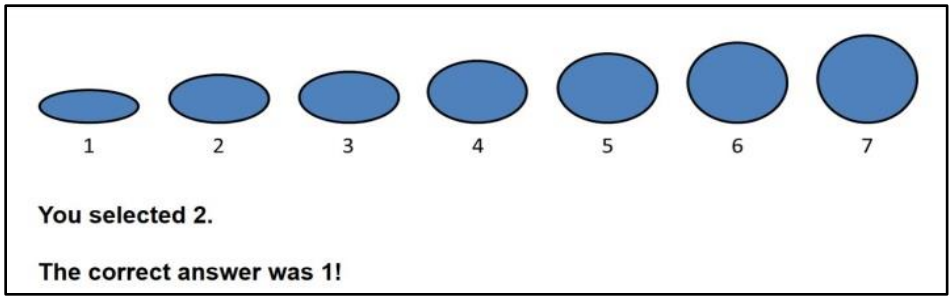

Figure 8. Example of the graphic feedback panel used in Experiment 4.

Results and Discussion

Initial analysis

We converted each of the numerical judgments participants made to the corresponding shape value of the ellipse chosen. We conducted an initial 2 (phase: training, transfer) x 7 (ellipse) x 3 (trial block) x 3 (transfer speed) ANOVA on judgments from the entire experiment, with Transfer speed a between-groups factor. The Phase main effect was significant, $F(1, 123) = 4.52$, $p = .035$, $\eta_{part}^2 = .035$, as was that for Ellipses, $F(6, 738) = 220.96$, $p < .001$, $\eta_{part}^2 = .64$. However, neither Block, $F < 1.00$, *ns*, $\eta_{part}^2 = .002$, nor Transfer speed, $F < 1.00$, *ns*, $\eta_{part}^2 = .008$, was significant. Significant interactions occurred for Phase x Ellipse, $F(6, 738) = 2.88$, $p = .009$, $\eta_{part}^2 = .02$; for Block x Ellipse, $F(12, 1476) = 2.58$, $p = .002$, $\eta_{part}^2 = .02$; and for Phase x Block

x Ellipse, $F(12, 1476) = 2.51$, $p = .003$, $\eta_{part}^2 = .02$. None of the interactions involving Transfer speed reached significance.

Given the initial significant Phase main, we analyzed Training and Transfer phase separately, as in Experiment 3. Figure 9 shows the pattern of mean judgments in the two phases.

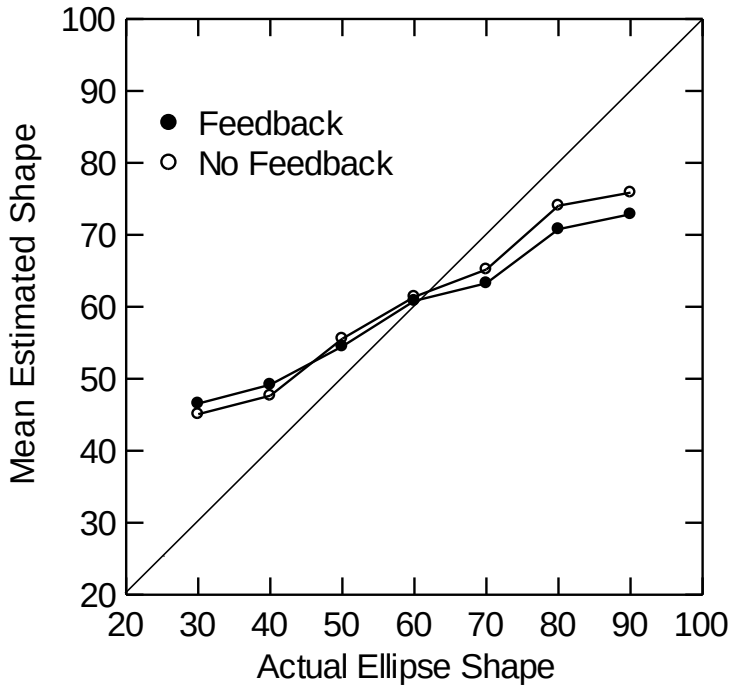

Figure 9. Mean judged ellipse shape versus actual shape in Experiment 4. Data from all speed comparison groups are combined. Error bars (*SEM*, calculated by the method of Franz & Loftus, 2012) are omitted because they fall within the size of the plotted points. The diagonal line represents perfect performance.

Training phase

For the Training phase, we subjected judgments to a 7 (ellipse) x 3 (block) x 3 (transfer speed) ANOVA, with repeated measures over Ellipse and Block. A significant main effect emerged only for Ellipse, $F(6, 738) = 120.93$, $p < .001$, $\eta_{part}^2 = .50$. Transfer speeds did not differ, $F < 1.00$, *ns*, $\eta_{part}^2 < .001$, nor was there a difference across Blocks, $F < 1.00$, *ns*, $\eta_{part}^2 =$

.006. The only significant interaction was Ellipse x Block, $F(12, 1476) = 3.59$, $p < .001$, $\eta_{part}^2 = .03$. None of the other interactions was significant.

The Ellipse linear trend was again strongly significant, $F(1, 123) = 324.44$, $p < .001$, $\eta_{part}^2 = .73$. Pairwise comparisons for the seven ellipses indicated 18 of the 21 significant mean judgment differences: Bonferroni-corrected $t(125) = 2.06$ to 17.12, $p = .041$ to $< .001$, Cohen's d from 0.18 to 1.53. There was no discernible pattern to the Ellipse x Block differences, however.

Transfer phase

The Transfer phase ANOVA showed a significant Ellipse main effect, $F(6, 738) = 158.06$, $p < .001$, $\eta_{part}^2 = .56$, but not for Block, $F(2, 246) = 1.19$, $p = .31$, $\eta_{part}^2 = .01$, or Transfer speed, $F(2, 123) = 1.07$, $p = .35$, $\eta_{part}^2 = .02$. Ellipse x Transfer speed was the only significant interaction, $F(12, 738) = 2.52$, $p = .003$, $\eta_{part}^2 = .04$.

As in the Training phase, the Ellipse linear trend was strongly significant, $F(1, 123) = 450.28$, $p < .001$, $\eta_{part}^2 = .79$. Mean comparisons for the seven ellipses showed that 19 of 21 were significant: Bonferroni-corrected $t(125) = 2.26$ to 18.60, $p = .04$ to $p < .001$, Cohen's $d = 0.28$ to 1.66. Clearly, on a group basis, participants differentiated and scaled the ellipses appropriately.

PCI analysis

Initial analysis. We analyzed PCI values for each participant for each block in the two experimental phases in a series of ANOVAs: (a) combined training and transfer data; (b) training phase alone; and (c) transfer phase alone. In a 2 (phase) x 3 (block) x 3 (transfer speed) ANOVA, significant main effects occurred for Phase, $F(1, 123) = 26.95$, $p < .001$, $\eta_{part}^2 = .18$, and Block, $F(2, 246) = 12.21$, $p < .001$, $\eta_{part}^2 = .09$. The Transfer speed main effect was not significant, $F(2, 123) = 1.74$, $p = .18$, $\eta_{part}^2 = .03$. No interaction was significant.

Training phase. In the Training phase, the Block effect was significant, $F(2, 246) = 11.71$, $p < .001$, $\eta_{part}^2 = .09$, but the Transfer speed effect was not, $F < 1.00$, *ns*, $\eta_{part}^2 = .02$. The interaction was also non-significant, $F < 1.00$, *ns*, $\eta_{part}^2 = .01$. Pairwise *t*-tests among Block means yielded differences between Block 1 ($M = 0.99$, $SD = 0.41$) and Block 2 ($M = 0.85$, $SD = 0.49$), $t(125) = 2.96$, $p = .004$, Cohen's $d = 0.27$, and between Blocks 1 and 3 ($M = 0.77$, $SD = 0.47$), $t(125) = 4.67$, $p < .001$, Cohen's $d = 0.42$, but not Blocks 2 and 3, $t(125) = 1.90$, $p = .06$, Cohen's $d = 0.17$. Note that the ordering of the block means was as predicted, although the pair-wise differences did not reach significance for Blocks 2 and 3, perhaps indicating a decreased effect of feedback.

Transfer phase. In the Transfer phase, the Block effect was again significant, $F(2, 246) = 3.18$, $p = .04$, $\eta_{part}^2 = .03$. Oddly, given the results of Experiment 3, the Transfer speed effect was significant, $F(2, 123) = 3.69$, $p = .03$, $\eta_{part}^2 = .06$. Pairwise *t*-test comparisons among Block means revealed a significant difference between Block 1 ($M = 1.07$, $SD = 0.42$) and Block 3 ($M = 0.97$, $SD = 0.43$), $t(125) = 2.21$, $p = .03$, Cohen's $d = 0.20$, and between Block 2 ($M = 1.06$, $SD = 0.45$) and Block 3, $t(125) = 2.12$, $p = .04$, Cohen's $d = 0.19$; Blocks 1 and 2 means did not differ significantly, $t(125) = .06$, $p = .95$, Cohen's $d = 0.006$.

Similar *t*-tests on mean PCI values for Transfer speeds yielded a significant difference between the 10 rpm ($M = 1.09$, $SD = 0.28$) and 15 rpm ($M = 0.93$, $SD = 0.30$) groups, $t(82) = 2.56$, $p = .01$, Cohen's $d = 0.28$, and between the 15 and 20 rpm ($M = 1.08$, $SD = 0.35$) groups, $t(82) = 2.22$, $p = .03$, Cohen's $d = 0.24$. The difference between the 10 rpm and 20 rpm group means was not significant, $t(82) = 0.09$, $p = .03$, Cohen's $d = 0.009$.

We infer from the PCI analyses that feedback on accuracy under the multiple-choice procedure improved perceptual performance to some degree. Transfer from the training speed to

the transfer speeds appeared to be somewhat variable, however, suggesting that transfer was not complete, perhaps due to limited numbers of feedback trials.

Comparison of Experiments 3 and 4

Except for response modes (scalar vs. multiple-choice), Experiments 3 and 4 were parallel, allowing a direct comparison of PCI values from Experiments 3 and 4. Figure 10 depicts the mean PCI values in training and transfer blocks for the two experiments. In passing, comparative tests of perceptual learning manipulations (e.g., Abernethy, Schorer, Jackson, & Hagemann, 2012) appear to be quite rare.

We first did an ANOVA on PCI values, using a 2 (experiment: 3, 4) x 2 (phase: training, transfer) x 3 (transfer speed: 10 rpm, 15 rpm, 20 rpm) x 3 (blocks) design, with repeated measures over Phase and Block factors. That analysis gave significant main effects for Phase, $F(1, 246) = 6.55$, $p = .01$, $\eta_{part}^2 = .03$; and Block, $F(2, 492) = 14.23$, $p < .001$, $\eta_{part}^2 = .06$. However, the main effects for Experiment, $F < 1.00$, *ns*, $\eta_{part}^2 = .004$, and Transfer speed, $F(2, 246) = 1.56$, $p = .21$, $\eta_{part}^2 = .01$, were not significant. Significant interactions occurred for Experiment x Phase, $F(1, 246) = 29.23$, $p < .001$, $\eta_{part}^2 = .11$; Experiment x Block, $F(2, 492) = 9.89$, $p < .001$, $\eta_{part}^2 = .04$; Phase x Block, $F(2, 492) = 9.71$, $p < .001$, $\eta_{part}^2 = .04$; and Phase x Transfer speed, $F(2, 246) = 6.41$, $p = .002$, $\eta_{part}^2 = .05$. Finally, the three-way Phase x Block x Transfer speed interaction was significant, $F(4, 492) = 3.11$, $p = .015$, $\eta_{part}^2 = .03$. Notably, effects involving Phase emerged as significant, as well as interactions with Experiment. Subsequently, we did separate ANOVAs for the training and transfer phases for the combined data sets for the two experiments.

Training phase. ANOVA for the Training phase produced significant main effects for Experiment, $F(1, 246) = 12.60$, $p < .001$, $\eta_{part}^2 = .05$, and Block, $F(2, 492) = 21.29$, $p < .001$, $\eta_{part}^2 = .08$, but not Transfer speed, $F < 1.00$, *ns*, $\eta_{part}^2 = .004$. Only the Experiment x Block interaction was significant, $F(2, 492) = 9.71$, $p < .001$, $\eta_{part}^2 = .04$.

Training phase mean comparisons showed a moderate advantage for the multiple-choice procedure (Experiment 4: $M = 0.95$, $SD = 0.28$) over scalar judgments (Experiment 3: $M = 0.99$, $SD = 0.31$. Mean PCI values across trial blocks also differed: The Block 1 mean ($M = 1.04$, $SD = 0.33$) was significantly higher than that of Block 2 ($M = 0.93$, $SD = 0.38$), $t(251) = 4.86$, $p < .001$, Cohen's $d = 0.03$, and significantly higher than for Block 3 ($M = 0.94$, $SD = 0.37$), $t(251) = 4.25$, $p < .001$, Cohen's $d = 0.02$. The means for Blocks 2 and 3 were not significantly different, $t(251) = 0.336$, $p = .74$, Cohen's $d = 0.02$. Mean PCI values differed between Experiments 3 and 4 ($M = 1.13$ [$SD = 0.36$] vs. 0.99 [$SD = 0.41$], respectively) at Training phase Block 1, $t(250) = 2.90$, $p = .004$, Cohen's $d = .18$, and Block 3 ($M = 1.06$ [$SD = 0.42$] vs. 0.77 [$SD = 0.47$]), $t(250) = 5.17$, $p < .001$, Cohen's $d = .33$. In both cases, the smaller Experiment 4 means indicated that multiple-choice performance exceeded scalar judgment performance. Block means did not differ significantly at Training phase Block 2 ($M = 0.86$ [$SD = 0.46$] vs. 0.85 [$SD = 0.49$]), $t(250) = 0.146$, $p = .88$, Cohen's $d = .01$, reflecting the dip in the curve at Block 2 in Experiment 3 (see Figure 10).

Transfer phase. The Transfer phase results yielded a significant main effect only for Transfer speed, $F(2, 246) = 4.63$, $p = .011$, $\eta_{part}^2 = .04$. Neither of the other two main effects was significant: Experiment, $F(1, 246) = 3.04$, $p = .08$, $\eta_{part}^2 = .01$; Block, $F(2, 492) = 1.69$, $p = 0.19$, $\eta_{part}^2 = .007$. No interaction was significant. The Transfer speed effect suggests incomplete transfer to novel speeds, an unexpected finding that deserves additional empirical attention. In

particular, mean PCI values for the 10 rpm group (*M* = 1.00, *SD* = 0.29) were higher than for either the 15 rpm (*M* = 0.92, *SD* = 0.31) or 20 rpm groups (*M* = 0.98, *SD* = 0.29).

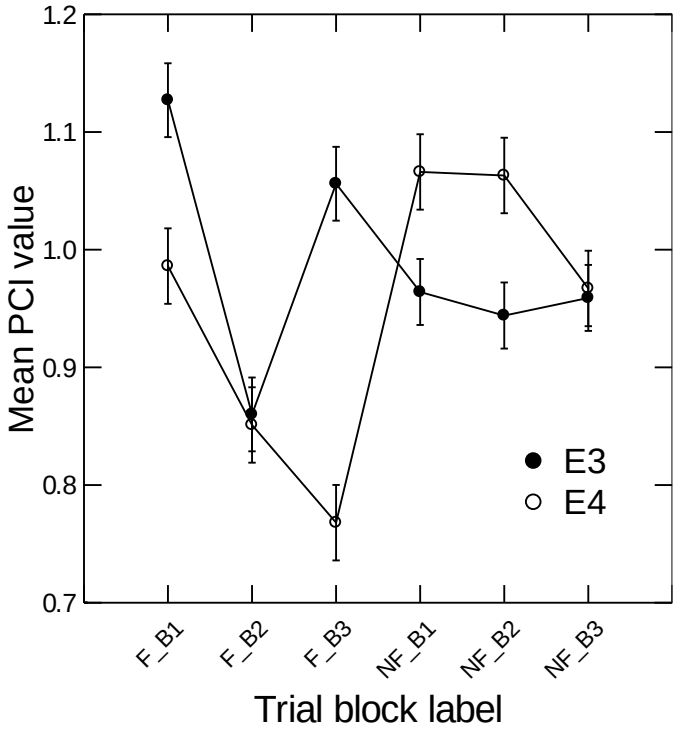

Figure 10. Mean perceptual calibration index (PCI) values across training with feedback on judgment accuracy in training blocks 1 - 3 (F_B1, F_B2, F_B3) and transfer trials with no feedback in transfer blocks 1 - 3 (NF_B1, NF_B2, NF_B3). Experiment 3 (E3) used scalar judgments; Experiment 4 (E4) used multiple-choice judgments. Error bars are ± 1 *SEM*, calculated using the method of Franz and Loftus (2012).

Figure 10 depicts mean PCI values across trial blocks in Experiments 3 and 4. Declining PCI values in training trials are consistent with predictions that feedback helping participants learn to use relevant information for differentiating and scaling ellipse shapes. However, transfer trial blocks means differ. In Experiment 3, transfer trial means remained at essentially the average performance level of the training trials, while the transfer means in Experiment 4 increased substantially from means in the training trials. Then, however, means in the transfer trials in Experiment 4 appear to decline, even in the absence of feedback. Consequently, the

effects of perceptual learning remain somewhat ambiguous. Further research on the problem is clearly warranted.

General Discussion

The experiments clearly document the existence of shape perception from friction-generated sound, at least within the ellipse shape family. We used ad hoc locally-constructed equipment, including a motor taken from equipment used in another project. We recorded sounds with a microphone originally intended for use in a discarded voice-recognition software package; the microphone had no label and we had no way of determining its characteristics. The online data collection dictated that sound stimuli be presented as mp3 files; we had no other option there. In the General Methods section, we commented that trial lengths could be defined either in terms of number of ellipse rotations or in terms of some fixed time length. We chose to restrict trials to three complete rotations of the ellipse. Thus, in Experiments 2, 3, and 4, trial lengths for 10 rpm rotations were 18 sec; for 15 rpm, 12 sec; and for 20 rpm, 9 sec. The absence of any rotation speed effect, however, argues that this choice had no meaningful influence on shape judgments.

Yet, even with all of these constraints and using technologically unsophisticated methodology, acknowledging the attendant noisy and likely imperfect fidelity of the acoustic signals, the fundamental effect was robust. Participants in all four experiments showed reliable differentiation and scaling of ellipse shapes from friction-generated sound.

Nevertheless, the results are decidedly exploratory and caution is warranted about generalizing beyond the conditions we used. We tested a circumscribed set of planar shapes, of a single material, with a single fixed major axis length, over a few rotation speeds, giving

participants restricted opportunity to sample the sound patterns, using a narrow range of response procedures. The analysis in the Appendix hints that other shapes should yield results consistent with those we obtained. The equivalence in shape judgments across speeds is consistent with the perspective that the relevant information for shape from sound is relational (e.g., for ellipses, the difference – or possibly the ratio – between frequency-intensity maxima and minima), as well as arguing that the restricted exposure to the sound patterns adequately supported shape perception. That relational hypothesis implies that sound patterns should invariantly specify other shapes (e.g., polygons, more complex curved shapes), made of other materials, of any size, rotating at any speed. All those variations pose testable research questions. Altering stimulus presentation parameters and testing with other response mechanisms are further empirical concerns.

While environmental sounds can arise from a variety of causes (Gaver, 1993a, b; Houix, Lemaitre, Misdariis, Susini, & Urdapilleta, 2012; Rochesso & Fontana, 2003), to the best of our knowledge, no one previously had considered the possibility that friction-generated sound might inform object shape differentiation and scaling (with the limited exception of work by Thoret et al., 2014, 2016). The analysis in the Appendix demonstrates a possible basis for such discriminability and scaling. The remarkable and surprising fact that emerged in all four experiments reported here is that humans reliably differentiated and scaled ellipse shape using acoustic information in friction-generated sound.

Experiment 1 documented that participants could distinguish and correctly order ellipse shapes varying in a singular shape parameter (the ratio of the minor axis length to major axis length), using sound patterns generated by friction between a fixed contactor and the rims of rotating ellipses. The non-significant effect of rotation speed in Experiment 2 hinted that some relational property or properties in the acoustic array supported the shape judgments.

In Experiments 1 and 2, individual differences were noticeable. Thus, in Experiment 3, we aimed to improve scalar shape judgments by giving feedback on judgment accuracy during training trials, then testing shape judgments without feedback in transfer trials, using the original training speed, plus two novel speeds. Experiment 4 paralleled Experiment 3, except using a multiple-choice procedure. Experiments 3 and 4 both replicated reliable differentiation and scaling seen in Experiments 1 and 2. Further, participants showed some improvement in shape judgments, with perhaps a moderate advantage for the multiple-choice procedure.

While the question originated by Kac (1966) remains somewhat unsettled, non-isospectrality across a delimited set of solid shapes does appear to yield acoustic array differences that empirically support shape discriminations. Earlier studies (e.g., Lakatos et al., 1992; Kunkler-Peck & Turvey, 2000) documented perception of shape from impact sounds. Kunkler-Peck and Turvey (2000) offered analyses based on vibratory physics to suggest that at least some shapes might be discriminable from impact sounds; their data supported that hypothesis. The present work adds to that comparatively limited corpus of data on perception of solid object shape from sound.

As noted in the introduction, the ecological (Gibsonian) perception research program rests on a priori stimulus array analysis for informative energy patterns, followed by empirical perceptual testing. Imperfect (or absent) perceptual performance suggests the opportunity for improved sensitivity via perceptual learning (E. Gibson, 1969). Here, prior analysis indicated that the friction-generated acoustic array might support ellipse shape perception. In our experiments, perceiving shape from friction-generated sound seems unlikely to be common experience, so the ability to make such judgments likely depended more on acoustic array characteristics than on experience. Performances observed varied widely in accuracy and

reliability, motivating perceptual learning manipulations in Experiments 3 and 4, results of which hinted at improved perceptual performance. As a package, then, the results of the experiments are consistent with the Gibsonian ecological perceptual framework.

The analysis in the Appendix indicated that frequencies and intensities of friction-generated sound vary as a function of the rotating ellipse shape, under specified constraints. That notion deserves a more direct test. Consequently, we anticipate developing synthesized acoustic patterns (cf., Thoret et al., 2014, 2016), in which intensities and frequencies change (either separately or combined), following the wave forms indicated in the Appendix, with varying amounts and kinds of noise added. If our analysis is correct, the resulting simulated sound patterns should support ellipse shape from sound perception.

Extension to additional shape families (e.g., polygons) becomes more feasible with synthesized sounds, as well. Thus, additional research questions become accessible, particularly the degree to which shape perception across shape families (e.g., ellipses vs. polygons). The mechanical recording arrangement we used cannot easily accommodate concavities in object perimeters. Synthesized sounds would allow such shapes to be explored empirically.

How far one might take such approaches is an open question, but environmental sound patterns may be richer sources of information than we imagine. For instance, Buckingham, Berkhout, and Glegg (1992) created visually-interpretable images from ambient noise in the ocean (e.g., created by wave movement). Fay (2009) argued that, because ambient noise has been an evolutionary constant in both aquatic and terrestrial environments, organisms are likely sensitive to such soundscapes. Consequently, humans might be capable of using more acoustic information than we currently know of to make spatial perceptual judgments and to guide action.

In all but Experiment 4, we used adjustment of a computer screen slider to indicate the relative minor-to-major ellipse axis length ratio. It is possible that the slider response was abstract enough that participants had difficulty expressing their judgments of shape, perhaps accounting for some of the judgment variability and inaccuracy. Alternative response mechanisms would be worth exploring. For example, one might present computer-generated ellipse shapes, such that the minor axis could be continuously adjusted relative to a constant major axis length (cf., Todd, 1985).

The stimuli used were of only a particular kind of friction-generated sound, from sheet steel ellipses with rims rotating against a sandpaper-coated contactor. The acoustic signal, therefore, was quite noisy (see Figure 2), and conceivably participants may have had difficulty extracting shape-related information from it, perhaps some more than others. Varying the nature of the contact (varying dimensions or materials), or using synthesized sounds, provides a means to test such a proposal. Arguing against that suggestion, however, is the patent finding that notable numbers of individuals made highly reliable judgments.

Some of the variance unaccounted in participants' responses for may have arisen from the high degree of task novelty. The perceptual learning manipulations in Experiments 3 and 4 aimed to reduce that variability and were successful to a moderate degree. This is a theme that deserves further examination. Remarkably (again), in all experiments a notable subset of individuals gave highly regular judgments.

Individual differences

While a majority of participants reliably discerned ellipse shape from sound, individual differences were manifest across the four experiments. The origins of those individual differences are unclear. One possible explanation is that we had no control over individual test

conditions, or of participants' motivational states or backgrounds. The circumstances under which individuals made judgments may also have contributed to the response variability (e.g., headphones vs. speakers, ambient noise levels, possible interruptions, competing tasks). Further, participant age ranges were quite large, up to 50 years. Additional demographic characteristics were unknown. Background differences (e.g., educational or occupational histories) may also have influenced performance. Finally, because participants were paid a minimal amount, we limited test session lengths.

To check potential effects of such issues, we replicated Experiment 1 with undergraduates (n = 17) in the laboratory. Thus, the age range was only 6 years, test conditions were standardized, and the motivational states, background, and other demographic elements were likely more homogeneous. Further, participants experienced more trials (four trial blocks vs. two) than the AMT participants. Results with the laboratory participants nicely replicated those from Experiment 1, with a large statistical effect for ellipse shape, a strong linear trend, and 16 of 21 pair-wise differences significant. Individual correlation magnitudes ranged from .19 to .88 (median, .62), with 15 of 17 (88%) significant ($p < .05$, n = 28 data points; 7 ellipses x 4 trial blocks). All outcomes were quite consistent Experiments 1– 4. Evidently, then, using AMT samples contributed minimally to the individual differences in performance we observed. The undergraduate study also validated the use of the AMT mechanism.

To conclude, the experiments reported here represent a novel theme in auditory perception, that of perceiving object shape from contact friction-generated sound. We readily acknowledge that many questions about these effects remain to be examined; we have attempted to suggest some productive avenues for such future research. Major theoretical significance of this work resides in the prospect of adducing additional evidence for commonalities across

sensory modes (e.g., vision and audition), as well as of illustrating the potential benefit (in the spirit of the Gibsonian ecological perceptual research program) of searching for informative structure in stimulus arrays as a source of testable perceptual hypotheses.

References

Abernethy, B., Schorer, J., Jackson, R. C., & Hagemann, N. (2012). Perceptual training methods compared: The relative efficacy of different approaches to enhancing sport-specific anticipation. Journal of Experimental Psychology: Applied, 18, 143–153. DOI: 10.1037/a0028452

Akay, A. (2002). Acoustics of friction. Journal of the Acoustical Society of America, 111, 1525-1548. DOI: 10.1121/1.1456514

Aurell, C. G. (1984). Note on Gibson's direct perception. Perceptual and Motor Skills, 58, 540-542.

Bocheva, N. (2009). Effect of planar cuts' orientation on the perceived surface layout and object's shape. Acta Psychologica, 131, 178-193.

Bresin, R., Delle Monache, S., Fontana, F., Papetti, S., Polotti, P., & Visell, Y. (2008). Auditory feedback through continuous control of crumpling sound synthesis. Proceedings of Sonic Interaction Design: Sound, Information and Experience. A CHI 2008 Workshop organized by COST Action IC0601, IUAV University of Venice , 2008, 23-28.

Buckingham, M. J., Berkhout, B. V., & Glegg, S. A. L. (1992). Imaging the ocean with ambient noise. Nature, 356, 327-329.

Buhrmester, M., Kwang, T., & Gosling, S. D. (2011). Amazon's Mechanical Turk: A new source of inexpensive, yet high-quality, data? Perspectives on Psychological Science, 6(1), 3-5. doi:10.1177/1745691610393980

Cabe, P. A. (2011). Haptic distal spatial perception mediated by strings: Haptic "looming." Journal of Experimental Psychology: Human Perception and Performance, 37, 1492–1511. DOI: 10.1037/a0024231

Cabe, P. A. (2010). Sufficiency of longitudinal moment of inertia for haptic cylinder length judgments. Journal of Experimental Psychology: Human Perception and Performance, 36, 373–394.

Cabe, P. A. (2013). Haptic distal spatial perception mediated by strings: Size at a distance and egocentric localization based on ellipse geometry. Attention, Perception, & Psychophysics, 75, 358–374. DOI 10.3758/s13414-012-0389-6

Cabe, P. A., & Hofman, L. L. (2012). Haptic distal spatial perception mediated by strings: Point of closest approach and bypass distance. Journal of Experimental Psychology: Human Perception and Performance, 38, 1328–1340.

Cabe, P. A., & Pittenger, J. B. (2000). Human sensitivity to acoustic information from vessel filling. Journal of Experimental Psychology: Human Perception and Performance, 26, 313-324.

Cabe, P. A., & Wagman, J. B. (2010). Characterizing perceptual learning using regression statistics: Development of a perceptual calibration index. American Journal of Psychology, 123, 253–267.

Crump, M. J. C., McDonnell, J. V., & Gureckis, T. M. (2013). Evaluating Amazon's Mechanical Turk as a tool for experimental behavioral research. Plos One, 8(3). doi:10.1371/journal.pone.0057410

Egan, E. J. L., Todd, J. T., & Phillips, F. (2011). The perception of 3D shape from planar cut contours. Journal of Vision, 11(12):15, 1–13. doi: 10.1167/11.12.15

Faul, F., Erdfelder, E., Buchner, A., & Lang, A.-G. (2009). Statistical power analyses using G*Power 3.1: Tests for correlation and regression analyses. Behavior Research Methods, 41, 1149-1160.

Fay, R. (2009). Soundscapes and the sense of hearing of fishes. Integrative Zoology, 4, 26-32. doi: 10.1111/j.1749-4877.2008.00132.x

Franz, V. H., & Loftus, G. R. (2012). Standard errors and confidence intervals in within-subjects designs: Generalizing Loftus and Masson (1994) and avoiding the biases of alternative accounts. Psychonomic Bulletin & Review, 19, 395-404.

Gaver, W. W. (1988). Everyday listening and auditory icons. (Unpublished doctoral dissertation). University of California, San Diego.

Gaver, W. W. (1993a). How do we hear in the world?: Explorations in ecological acoustics. Ecological Psychology, 5, 285-313.

Gaver, W. W. (1993b). What in the world do we hear?: An ecological approach to auditory event perception. Ecological Psychology, 5, 1-29.

Gescheider, G. A. (1997). Psychophysics: The fundamentals. (2nd. ed.). Mahwah, NJ: Erlbaum.

Gibson, E. J. (1969). Principles of perceptual learning and development. New York: Appleton-Century-Crofts.

Gibson, J. J. (1966). The senses considered as perceptual systems. Boston: Houghton-Mifflin.

Gibson, J. J. (1979). The ecological approach to visual perception. Boston: Houghton-Mifflin.

Giordano, B. L. (2005). Sound source perception in impact sounds. (Unpublished doctoral dissertation). University of Padua, Padua, Italy.

Grieser, D., & Maronna, S. (2013). Hearing the shape of a triangle. arXiv:1208.3163 [math.SP]

Griffin, D. R. (2001). Return to the magic well: Echolocation behavior of bats and responses of insect prey. BioScience, 51, 555-556.

Hezari, H., Lu, Z., & Rowlett, J. (2016). The Neumann isospectral problem for trapezoids. arXiv:16001.00774v1 [math.SP]

Holden, C. J., Dennie, T., & Hicks, A. D. (2013). Assessing the reliability of the M5-120 on Amazon's Mechanical Turk. Computers in Human Behavior, 29, 1749-1754. doi:10.1016/j.chb.2013.02.020

Houben, M. M. J., Kohlrausch, A., & Hermes, D. J. (2004). Perception of the size and speed of rolling balls by sound. Speech Communication, 43, 331–345. doi:10.1016/j.specom.2004.03.004

Houix, O., Lemaitre, G., Misdariis, N., Susini, P., & Urdapilleta, I. (2012). A lexical analysis of environmental sound categories. Journal of Experimental Psychology: Applied, 18, 52-80. DOI: 10.1037/a0026240

Houix, O., McAdams, S., & Caussé, R. (1999). Auditory categorization of sound sources. In M. A. Grealey & J. A. Thomson (Eds.), Studies in Perception and Action V (pp. 47-51). Mahwah, NJ: Erlbaum.

Kac, M. (1966). Can one hear the shape of a drum? American Mathematical Monthly. 73 (4, part 2): 1-23

Kirkwood, B. C. (2007). Information from impact sounds: Normal and impaired hearing. (Unpublished doctoral dissertation). Technical University of Denmark, Kongens Lyngby, Denmark.

Kunkler-Peck, A. J., & Turvey, M. T. (2000). Hearing shape. Journal of Experimental Psychology: Human Perception and Performance, 26, 279-294.

Lakatos, S., McAdams, S., & Caussé, R. (1997). The representation of auditory source characteristics: Simple geometric form. Perception & Psychophysics, 59, 1180-1190.

Lappin, J. (1995). Visible information about structure from motion. In W. Epstein & S. Rogers (Eds.), Perception of space and motion (pp. 165-199). New York, NY: Academic.

McCrae, J. (2014). Planar section representations of 3d shape. (Unpublished doctoral dissertation.) University of Toronto, Toronto, Ontario, Canada.

Michaels, C., & Carello, C. (1981). Direct perception. New York: Appleton-Century-Crofts.

Neuhoff, J. G. (2001). An adaptive bias in the perception of looming auditory motion. Ecological Psychology, 13, 87-110.

Neuhoff, J. G. (2016). Looming sounds are perceived as faster than receding sounds. Cognitive Research: Principles and Implications 1:15. DOI: 10.1186/s41235-016-0017-4.

Neuhoff, J. G., Schott, S. A., Kropf, A. J., & Neuhoff, E. M. (2014). Familiarity, expertise, and change detection: Change deafness is worse in your native language. Perception. 43, 219-222.

Norman, J. F., Phillips, F., Cheeseman, J. R., Thomason, K. E., Ronning, C., Behari, K., Kleinman, K., Calloway, A. B., & Lamirande, D. (2016). Perceiving object shape from specular highlight deformation, boundary contour deformation, and active haptic manipulation. PLoS ONE 11(2): e0149058. doi:10.1371/journal.pone.0149058

Paolacci, G., Chandler, J., & Ipeirotis, P. G. (2010). Running experiments on Amazon Mechanical Turk. Judgment and Decision Making, 5(5), 411-419.

Rochesso, D., & Fontana, F. (Eds.). (2003). The sounding object. Venice, Italy: Edizioni di Mondo Estremo.

Rosenblum, L. D., & Robart, R. L. (2007). Hearing silent shapes: Identifying the shape of a sound-obstructing surface. Ecological Psychology, 19, 351–366.

Sedgwick, H. A. (1973). The visible horizon: A potential source of visual information for the perception of size and distance. Dissertation Abstracts International, 34, 1301-1302B. (UMI No. 7322530).

Stevens, S. S. (1975) Psychophysics: Introduction to its perceptual, neural, and social effects. New York, Wiley.

Thoret, E., Aramaki, M., Bringoux, L., Ystad, S., & Kronland-Martinet, R. (2016). Seeing circles and drawing ellipses: When sound biases reproduction of visual motion. PLoS ONE, 11(4), e0154475. April 27, 2916. DOI:10-1371/journal.pone.0154475.

Thoret, E., Aramaki, M., Kronland-Martinet, R., Velay, J.-L., & Ystad, S. (2014). From sound to shape: Auditory perception of drawing movements. Journal of Experimental Psychology: Human Perception and Performance, 40, 983-994.

Todd, J. T. (1985). Perception of structure from motion: Is projective correspondence of moving elements a necessary condition? Journal of Experimental Psychology: Human Perception and Performance, 11, 689-710.

Todd, J. T. (1995). The visual perception of three-dimensional structure from motion. In W. Epstein & S. Rogers (Eds.), Perception of space and motion (pp. 201-226). New York, NY: Academic.

Turvey, M. T., Solomon, H. Y., & Burton, G. (1989). An ecological analysis of knowing by wielding. Journal of the Experimental Analysis of Behavior, 52, 387–407. doi:10.1901/jeab.1989.52-387

Withagen, R., & Caljouw, S. R. (2011). Aging affects attunement in perceiving length by dynamic touch. Attention, Perception, & Psychophysics, 73, 1216–1226. DOI 10.3758/s13414-011-0092-z

Wong, K.-Y. K. (2001). Structure and motion from silhouettes. (Unpublished doctoral dissertation.) University of Cambridge, Cambridge, England.

Appendix

Shape information from friction-generated sound

Friction generates sound in many familiar situations, from wet shoe soles squeaking on a floor to the bowing of a violin string. The intricacies of the dynamics of sound generation by contact friction between surfaces sliding relative to one another are complex and beyond the scope of this paper (for an overview, see Akay, 2002). However, to a reasonable approximation, friction-generated sound is a function of the relative velocity of one surface against the other and of elements affecting friction at the point of contact. Standard texts describe those elements as (a) the normal force between the two objects, (b) contact area, and (c) surface roughness of the contacting surfaces.

Consider the scenario shown in Figure 1: A contactor attached to a pivoting cantilevered beam is free to rotate about a pivot. At the non-pivoting end of the arm, the contactor rests against the rim of an elliptical disk rotating about its center. The contactor has a circular cross-section, with a sheet of sandpaper on the contactor surface. Normal force (e.g., weight of the contactor against the ellipse rim), surface roughness, and contact area are essentially constant.

In general, tangential velocity of any point on a rotating body is a function of angular velocity and the point's radial distance from the center of rotation. Points along the ellipse perimeter differ in that radial distance as a function of the elliptical shape. With the ellipse rotating at a constant angular velocity, tangential velocity at the point of contact with the contactor varies with the angular position of the point on the perimeter of the ellipse. The velocity of the ellipse against the contactor is the tangential velocity at the point of contact. What we want to show is the pattern of tangential velocity changes as a function of ellipse shape, as the ellipse rotates at a constant angular velocity. Thus, we need to find tangential velocity as a

function of angular velocity and the radial distance from the center of rotation to the contact point.

For an ellipse with its major axis coincident with the horizontal axis of a Cartesian coordinate system and with the ellipse center at the coordinate system origin, the polar equation for an ellipse is

$$r(\theta) = \frac{a\,b}{\sqrt{(b\,COS(\theta))^2+(a\,SIN(\theta))^2}} \qquad \text{(A1)}$$

where $r(\theta)$ is the radial distance from the center of the ellipse at angle θ from the horizontal coordinate axis; a and b are lengths of the ellipse major and minor axes, respectively. We define the minor axis length, b, as some proportion, p, of the major axis length, a. The variable, p, then is a shape parameter for the ellipse. Substituting pa for b in equation (A1) and simplifying alters equation (A1) to

$$r(\theta) = \frac{p\,a^2}{\sqrt{(p\,a\,COS(\theta))^2+(a\,SIN(\theta))^2}} \qquad \text{(A2)}$$

Tangential velocity, V_r, of any point along the perimeter of the ellipse is the product of the ellipse's angular velocity, ω, and radial distance between the center of rotation and that point: $V_r = \omega\, r(\theta)$. Substituting the expression for $r(\theta)$ from equation (A2), and simplifying by noting that $COS(\theta)^2 = 1 - SIN(\theta)^2$, yields

$$V_r = \omega\left[\frac{p\,a}{\sqrt{(1-p^2)\,SIN(\theta)^2+\,p^2}}\right] \qquad \text{(A3)}$$

Tangential velocity at any point on the ellipse rim is therefore a function of angular velocity of the rotating ellipse, the shape parameter (i.e., the ratio of the minor axis length to the major axis length), and the angle between the coordinate axes and a line from the center of rotation through the selected point on the ellipse rim. The relevant relationship is between the

position on the ellipse rim defined by θ and the shape parameter, p, with ω and a scaling variables.

Solving equation (A3) for a gives

$$a = \frac{V_r \sqrt{(1-p^2)\, SIN(\theta)^2 + p^2}}{p\ \omega} \qquad \text{(A4)}$$

Taking the derivative of equation (A3) with respect to θ results in the expression

$$\frac{dVr}{d\theta} = -\frac{a\ p\ \omega\ (p^2-1) SIN(\theta)\ COS(\theta)}{[(1-p^2)\, SIN(\theta)^2 + p^2]^{3/2}} \qquad \text{(A5)}$$

Substituting the expression for a from equation (A4) into equation (A5) and simplifying yields

$$\frac{dV_r}{d\theta} = \frac{V_r\,(1-p^2)\, SIN(\theta)\ COS(\theta)}{(p^2-1)\, SIN(\theta)^2 - P^2} \qquad \text{(A6)}$$

Solving for p, the ellipse shape parameter, and noting that p can only be positive (thus, only the positive root of the quadratic is meaningful), produces

$$p = \frac{\sqrt{SIN(\theta)\ [V_r\ COS(\theta)\ d\theta + SIN(\theta) dV_r]}}{\sqrt{V_r\ SIN(\theta)\ COS(\theta)\ d\theta + [SIN(\theta)^2 - 1]\ dV_r}} \qquad \text{(A7)}$$

We conclude from equation (A7), therefore, that p, the ellipse shape parameter, is defined in terms of the momentary value of tangential velocity, V_r, at a radial position on the rim of the ellipse defined by θ , and the rate of change in tangential velocity, dV_r, as a function of the rate of change in the angle, $d\theta$. Because friction-generated sound is a function of tangential velocity, it follows that changes in friction-generated sound yield auditory information for ellipse shape.

Note that, because they define tangential velocity, angular velocity (rotation speed, ω) and major axis length, a, are still implicit in equation (A7). Those elements suggest that, within a family of ellipses defined by a constant major axis length, confusions could result between ellipses of different shape rotating at different angular velocities (rotation speeds).

Equation (A7) indicates that information for ellipse shape exists in the friction-generated acoustic array and yields the primary hypothesis of the present research, that ellipse shape might

be perceptible using the friction-generated sound of a contactor sliding along the perimeter of the ellipse, as the ellipses rotate at a constant angular velocity. Note that ellipse major axis length, a, and angular velocity, ω, are not factors in equation (A7), implying that ellipse shape from friction-generated sound is invariant with respect to ellipse size and to angular velocity (i.e., rotation speed), leading to the additional hypothesis that shape discriminability should be equivalent across differing (but constant) rotation speeds and ellipse sizes.

Figure A1 shows ellipse tangential velocity as a function of degree of rotation. Figure A2 plots rate of change of tangential velocity as a function of degree of rotation. In both figures, angular velocity, ω, and ellipse major axis, a, have been set to unity as scaling variables. Clearly, from the plots, the curves are visibly different, again suggesting that friction-generated sound differences could provide a basis for discriminating ellipse shape differences.

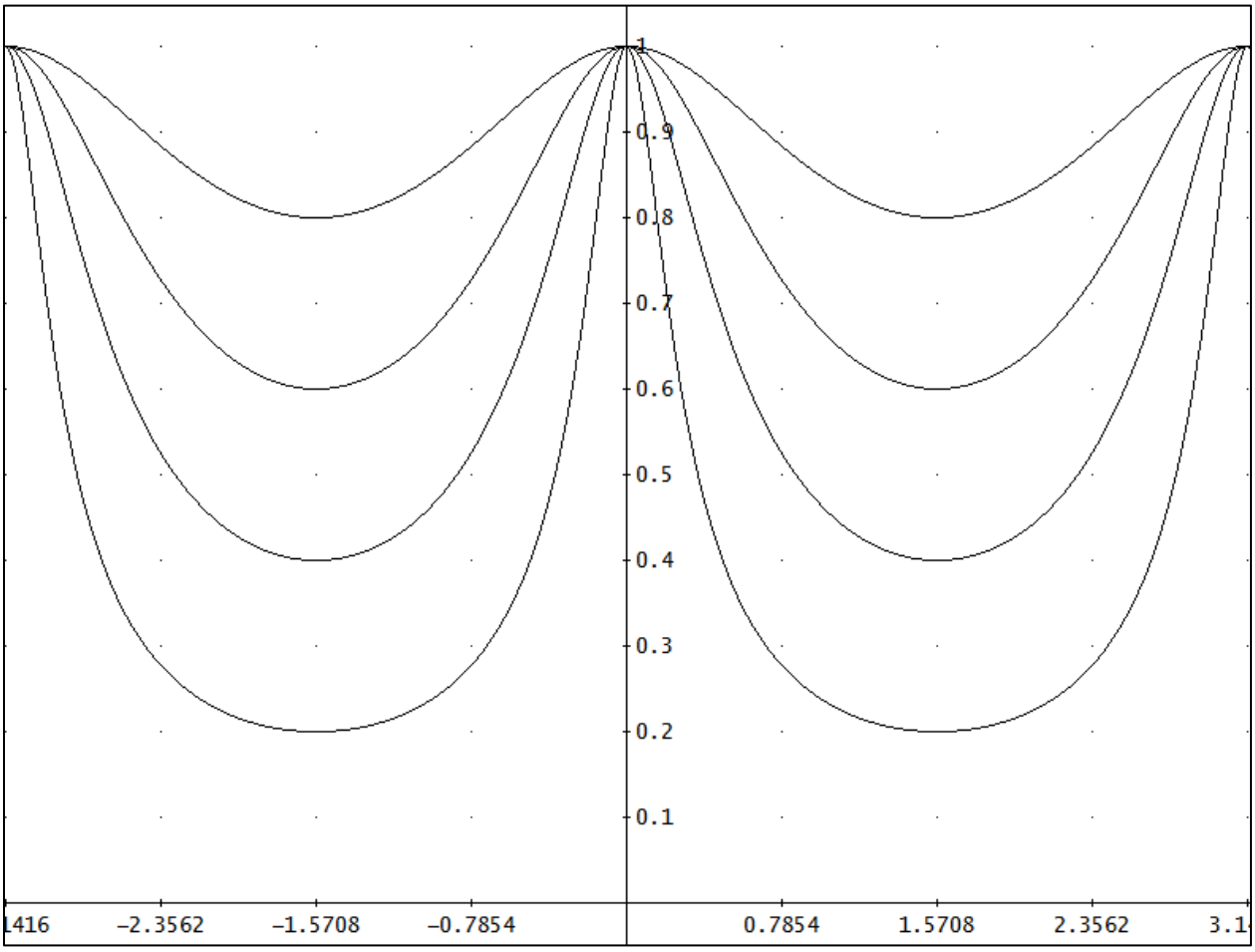

Figure A1. Plots of angular velocity as a function of degree of rotation (in radians), for ellipses with minor-to-major axis length ratios (expressed as percentages) of 20, 40, 60, and 80% (bottom to top). Angular velocity and major axis length are scaling factors set to unity for the calculations to produce these graphs.

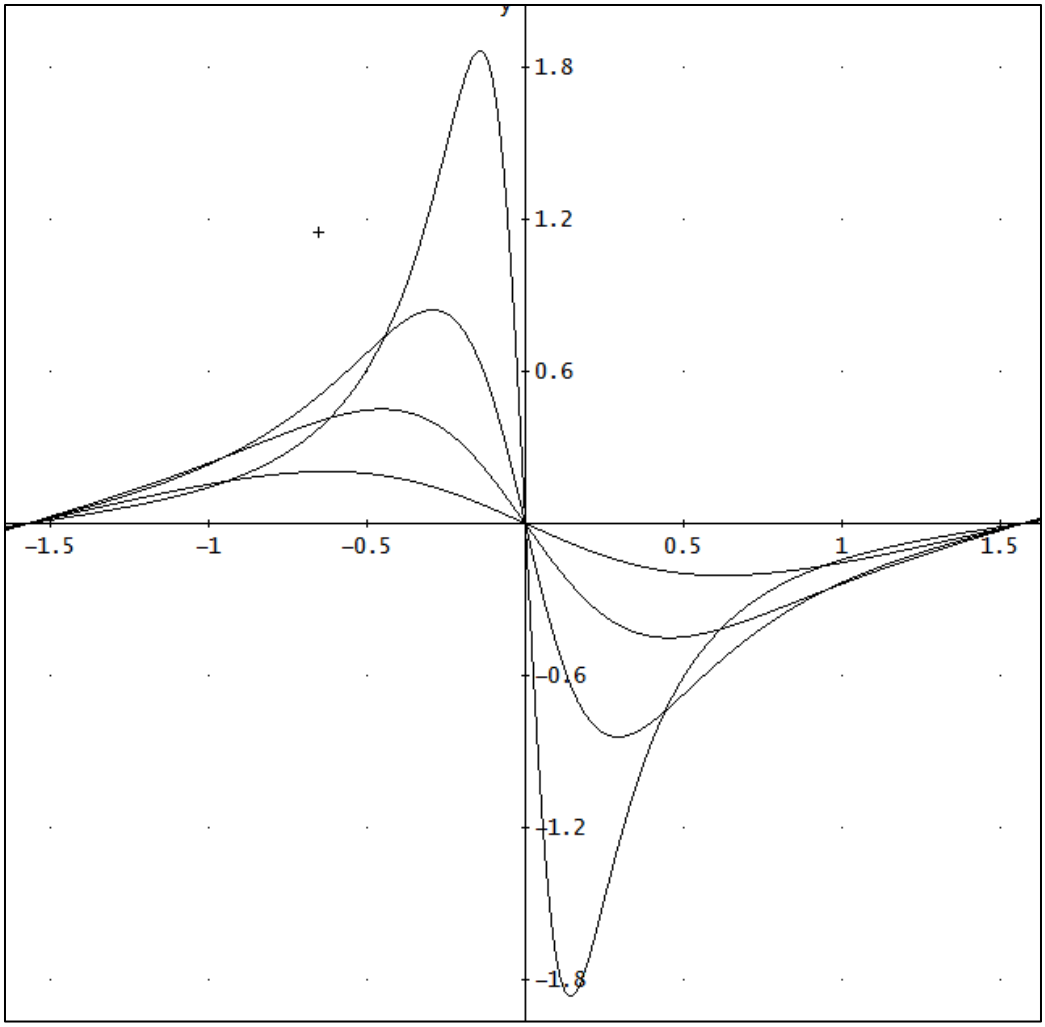

Figure A2. Plots of rates of change in angular velocity as a function of degree of rotation (in radians), for ellipses with minor-to-major axis length ratios (expressed as percentages) of 20, 40, 60, and 80% (top to bottom). Angular velocity and major axis length are scaling factors set to unity for the calculations to produce these graphs.